IEEE Access
Multidisciplinary ⋮ Rapid Review ⋮ Open Access Journal

Received 1 March 2026, accepted 19 April 2026, date of publication 23 April 2026, date of current version 29 April 2026.

Digital Object Identifier 10.1109/ACCESS.2026.3687029

RESEARCH ARTICLE

Resident Change Detection Using Electricity and Gas Metering Data

JONGIN KIM[1], (Student Member, IEEE), DONG SIK KIM[1], (Senior Member, IEEE), YOUNG MO CHUNG[2], (Member, IEEE), AND BEOM JIN CHUNG[3]

[1]Division of Semiconductor and Electronics Engineering, Hankuk University of Foreign Studies, Yongin-si, Gyeonggi-do 17035, Republic of Korea
[2]Department of Electronics and Information Engineering, Hansung University, Seoul 02876, Republic of Korea
[3]Research Center of Electrical and Information Technology, Seoul National University of Science and Technology, Seoul 01811, Republic of Korea

Corresponding author: Dong Sik Kim (dskim@hufs.ac.kr)

This work was supported by Korea Institute of Energy Technology Evaluation and Planning (KETEP) through the Ministry of Climate, Energy and Environment (MCEE) of Republic of Korea under Grant RS-2023-00236325. The work of Young Mo Chung was supported by Hansung University.

ABSTRACT As smart meter technology advances, advanced metering infrastructure (AMI) enables the collection of high-resolution energy consumption data, such as 15-minute interval electricity and gas usage. While anomaly detection studies have primarily focused on industrial infrastructure, the challenge of identifying specific residential events, such as resident changes, in an unsupervised manner remains largely unaddressed. In this paper, we propose an unsupervised framework to detect the month of a resident change by interpreting significant prediction errors from a deep learning model as anomalies. Our framework utilizes a gated recurrent unit and fully connected layer (GRU-FC) model to predict both monthly consumption patterns and amounts. For training and validation, we used electricity and gas datasets collected from 750 households in Seoul, Republic of Korea, using AMI. These datasets contain ground-truth labels for the actual resident change dates that occurred in the households in 2024. To prepare the datasets for training the GRU-FC model, an efficient outlier removal scheme was developed based on vector quantization. Combined-loss and complementary decision schemes were also employed to jointly leverage pattern and amount features for both electricity and gas data. When only electricity data was used, the detection accuracy was 80.37%, which increased significantly to 89.19% when electricity and gas datasets were used together. This study not only demonstrates the practical feasibility of detecting resident changes but also highlights the effectiveness of a multi-source, prediction-based approach for general time-series anomaly detection.

INDEX TERMS Advanced metering infrastructure, anomaly detection, gated recurrent unit, outlier removal, resident change detection.

I. INTRODUCTION

To mitigate climate change, the global energy system is undergoing a transition centered on the proliferation of distributed energy resources (DERs), such as solar photovoltaic systems, energy storage systems, and electric vehicles. During this transition, digitalization for collecting and utilizing energy data is emerging as a crucial facilitator [1]. Advanced metering infrastructure (AMI) provides the foundational platform for this digital transformation, delivering high-resolution time-series data on energy consumption [2], [3], [4], [5]. Additionally, as grid integration of various DERs increases, leveraging energy data collected through AMI together with other distributed resource information and meteorological data becomes increasingly important. This leveraging necessitates an evolution beyond the simple collection and storage of energy data toward sophisticated frameworks for data sharing and utilization that support advanced demand flexibility services, such as demand response (DR) programs and virtual power plants that harness distributed resources [6], [7], [8].

Energy suppliers have traditionally deployed AMI with the primary goal of revenue protection, which was achieved by cutting expenses from manual meter reading and preventing

The associate editor coordinating the review of this manuscript and approving it for publication was Bang L. H. Nguyen.

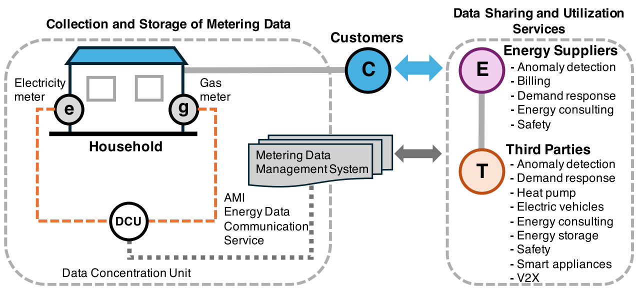

FIGURE 1. **Collection and storage of electricity and gas consumption metering data. Energy data sharing and utilization services, in which the metering data is used, are also summarized.**

electricity theft, and have expanded their use of data to include operations such as distribution system management and DR [9], [10], [11]. However, with the expanding share of renewable energy generation driven by the energy transition, the resulting grid instability has made securing flexibility resources increasingly critical. This necessity calls for the expanded participation not only of energy suppliers but also of third parties, such as appliance manufacturers, electric vehicle manufacturers and charging operators, and energy service providers of virtual power plants [12].

Especially in the area of data sharing and utilization services, there is growing interest in real-time monitoring and analysis, such as pollution control [13], leakage [14], energy consulting [5], and energy theft [15], [16], [17], [18]. Here, to provide reliable and high-quality services, research has been conducted to combine electricity and water metering data [19], or even gas metering data [20]. Fig. 1 summarizes various services in the data sharing and utilization area with a model of data collection and storage for electricity and gas consumption.

To develop and operate these sharing and utilization services reliably, third parties require access to and use of not only the energy data collected through AMI, but also various personal information related to customers. However, because such personal information is not readily accessible, it should be indirectly inferred from AMI data. Here, *anomaly detection* is a technique that can efficiently infer the necessary information. The ability to detect anomalies is crucial for identifying specific events that alter a household energy profile, such as a *resident change*. If this change is not updated immediately, the following problems may occur. Delayed updates may make it difficult to provide accurate information about routine inspections, emergency repairs, or welfare discount programs to new residents. Furthermore, privacy and data rights violations can occur, as the consumption data of new residents may be exposed to former residents, potentially leading to disputes over billing and liability. Hence, it is very important to promptly detect when a resident change occurs and notify residents whose official updates have not yet been completed.

For time-series anomaly detection, deep learning-based unsupervised learning methodologies that capture normal patterns without labeled data have been extensively researched [21]. These approaches are generally categorized into reconstruction-based methods utilizing autoencoders and prediction-based methods employing recurrent neural network (RNN) architectures. Reconstruction-based models learn the overall distribution of data and detect anomalies through reconstruction error, while prediction-based models capture temporal continuity in the data and identify anomalies through prediction errors [22]. Several studies have been conducted on time-series anomaly detection. Gong et al. [23] introduced multi-timestamp stacking and random shuffling to enhance training robustness using a gated recurrent unit (GRU)-AutoEncoder in large-scale traffic load anomaly detections using data from a cellular service provider. Zhao et al. [24] proposed a bidirectional structure and hierarchical probabilistic modeling to capture long-range dependencies using a bidirectional deep variational recurrent neural network (bi-DVRNN). Choi et al. [25] developed a generative adversarial network (GAN)-based framework that transforms multivariate time series into distance images to detect and localize anomalies. Malhotra et al. [26] proposed a long short-term memory (LSTM)-based encoder-decoder architecture that reconstructs multivariate time series and detects anomalies based on reconstruction errors. Hundman et al. [27] utilized LSTMs combined with nonparametric dynamic thresholding to detect anomalies in spacecraft telemetry data. These studies typically focus on high-frequency, large-volume data from industrial systems, and are often designed for real-time monitoring.

Deep learning methods can also be used to detect resident changes, with the framework focusing on the home environment by analyzing residents' consumption patterns on a monthly basis and detecting changes based on non-real-time event detection methods. However, resident change events exhibit unique characteristics that distinguish them from the cases typically addressed in conventional anomaly detection research. First, changes in consumption patterns resulting from resident transitions may not exhibit clear signals and can be confounded by other sources of variability. Second, obtaining large-scale labeled datasets specifying the precise timing of resident changes is highly challenging in practice, which limits the applicability of supervised learning approaches [17]. Third, the presence of atypical transitional state patterns before and after a move makes it difficult to accurately estimate change points using simple pattern change detection.

Furthermore, most of these anomaly detection studies used time-series data collected from non-residential environments, such as industrial facilities, large-scale system operations, and synthetic data. Such data differ significantly in structure and granularity from household metering data, which are measured at 15-minute intervals. In addition, validating models against real-world data is often hindered by the practical difficulty of obtaining datasets with precisely defined and verified labels for specific events, such as resident changes.

In this paper, we propose an unsupervised deep learning-based framework to detect the month of a resident change using high-resolution electricity and gas energy datasets collected from 750 real-world households through AMI. Notably, these datasets contain ground-truth labels for actual resident changes that occurred within these households, enabling rigorous validation of our unsupervised framework against real-world events. First, our approach analyzes electricity and gas datasets independently, leveraging two key features from each source: the monthly consumption pattern and the total monthly consumption amount. A GRU-based model predicts these features, and significant prediction errors are interpreted as anomalies indicating a resident change. For the final decision, we then employ a complementary strategy that integrates findings from both energy datasets. With this method, we decide that a resident change has occurred if a significant anomaly is detected in either the electricity analysis or the gas analysis. This multi-source strategy enhances detection robustness by capturing diverse behavioral changes specific to each energy type.

This paper is organized as follows. In Section II, we describe the dataset construction and preprocessing schemes for outlier removal. In Section III, we introduce prediction models based on deep learning and the proposed resident change detection method. Section IV presents simulation results for the performance evaluation. In Section V, we discuss several issues related to the detection failures. The paper is concluded in the last section.

II. METERING DATASETS OF ELECTRICITY AND GAS CONSUMPTION

In this section, we first describe a metering dataset that includes electricity and gas consumption, and then introduce an outlier removal method based on vector quantization (VQ) to prepare the dataset for conducting the resident change detection using deep learning.

A. MONTHLY PATTERNS AND AMOUNTS

To develop a resident change detection method and evaluate its performance, consumption data for both energy sources of electricity and gas were collected at 15-minute intervals from 750 apartment households in Seoul, Republic of Korea, using AMI over a one-year period from January to December 2024 (Fig. 1, Seoul City Gas Co. Ltd., Seoul, Republic of Korea, www.seoulgas.co.kr). For each household, 96 energy consumption readings were recorded per day for each energy source, resulting in a total of 26,352,000 values per source. Among the 750 households, we investigated the date when the actual resident changed residence due to moving, and found that 58 households relocated in 2024. Prior to training, data contamination caused by communication errors in the metered data was corrected using appropriate schemes [3], [4].

The monthly energy consumption pattern for each household is defined as follows. Electricity or gas consumption measured daily can be expressed as a 96-dimensional vector due to the 15-minute interval metering. For each household, the *monthly pattern* is defined as the average of daily vectors over a month and normalized to emphasize relative differences between patterns. Here, min-max normalization is applied so that all elements of each monthly pattern fall within the range [0, 1]. Note that the monthly pattern is also a 96-dimensional vector and each household has 12 monthly patterns for each energy source. The energy consumption amount is defined in a similar manner. For each household, the monthly energy consumption amount is defined as the sum of all elements of the daily vectors over a month. Hence, the *monthly amount* is a scalar and each household also has 12 monthly amounts for each energy source.

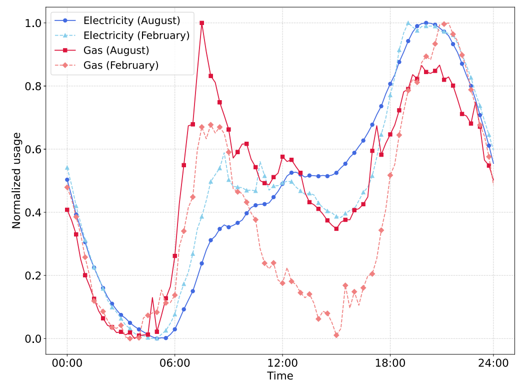

FIGURE 2. Monthly pattern examples for the electricity and gas consumption for a household. In general, energy consumption decreases in the early morning and increases in the evening. For gas, the monthly pattern curve exhibits noisy characteristics. This suggests that the number of gas-using devices is small and their usage is intermittent.

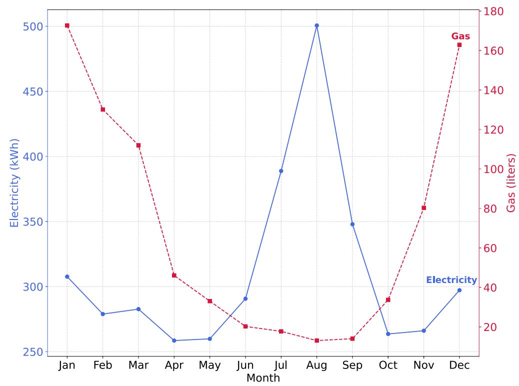

FIGURE 3. Monthly amount examples for the electricity and gas consumption for a household. Electricity consumption peaks in August, a summer month, due to the use of air conditioners. Conversely, gas consumption increases in winter for heating purposes.

An example of the monthly patterns for the electricity and gas consumption for a household is shown in Fig. 2. In general, energy consumption decreases in the early morning and increases in the evening. However, each household may exhibit a variety of meaningful consumption patterns reflecting lifestyle. Fig. 3 shows the monthly amounts for the same household in Fig. 2, for both electricity and gas. Comparative observations of these amounts are commonly used to differentiate electricity consumers.

B. CONSISTENCY AND OUTLIER REMOVAL

To examine the properties of the monthly pattern for a given energy type, we first aggregated the 96-dimensional vectors representing the monthly patterns of all households and performed a k-means clustering analysis. We applied several methods to determine the appropriate number of clusters for our dataset, including elbow curves, information-theoretic criteria, silhouette method, gap statistic, and β-compensation distortion [28], [29], [30], [31], [32]. However, the results indicated that none of the applied criteria provided a clear number of clusters. This collective ambiguity suggests that monthly patterns are not composed of a finite number of discrete clusters, but can take a variety of forms across households. Hence, the monthly patterns may exhibit unique characteristics for each household, and examining these patterns may allow for the identification of each household. Note that, if the number of clusters is small, then it will be difficult to distinguish households solely by observing the patterns.

Let us introduce the notion of a *consistency assumption* that the unique pattern of each household does not change significantly from month to month. If the current monthly pattern, which is predicted based on past patterns, does not differ substantially from the actual current pattern, then it can be determined that the same residents are consuming energy. Conversely, if there is a large discrepancy in the predicted and actual patterns, there may have been a change in the type of energy-consuming residents. Hence, we can detect the resident changes by predicting and comparing the monthly patterns under the assumption of temporally consistent patterns.

To accurately predict the monthly patterns of electricity and gas, we employed a deep learning technique. To properly train the prediction models, we preprocessed the dataset to remove outliers that exhibit temporal inconsistencies in monthly patterns.

A simple scheme to remove outlier households that do not follow the consistency assumption is as follows. We first represent the monthly patterns of all households using VQ with N representative patterns or *centroids*, to briefly capture their overall characteristics in the 96-dimensional space [33]. Here, N is a positive integer and the centroids are designed from the generalized Lloyd-Max algorithm, which is equivalent to iteratively clustering the dataset with the k-means algorithm, by minimizing the empirical distortion [34].

We assume that outlier households are primarily characterized by high pattern diversity, meaning their patterns vary significantly from month to month. From the VQ results, we can quantify this concept for each household by counting the minimal number of centroids used to quantize its 12 monthly patterns. As the number of used centroids increases, the household exhibits greater pattern diversity and may not follow the consistency assumption, identified as an outlier. This method for identifying outlier households based on monthly patterns is summarized as follows.

Outlier Households against the Consistency Assumption:

0) Design N centroids using the monthly patterns of all households based on VQ; set the threshold T_o.
1) For each household, quantize its12 monthly patterns and count the number of used centroids.
2) If the number of used centroids exceeds T_o, then the household is regarded as an outlier.

Fig. 4 shows the histograms of the number of used centroids for both electricity and gas consumption, where $N = 10$. We can observe that the gas patterns have higher diversity than the electricity patterns do. Specifically, 37 households show a high degree of consistency in their electricity consumption, where all 12 monthly patterns belong to a single cluster. In other words, the number of used centroids is 1 for these households. In contrast, for the gas case, only 4 households exhibit this level of consistency. Furthermore, the maximum number of households for electricity occurs when 3 centroids are used (223 households), whereas for gas, the maximum occurs at a larger number of 4 used centroids (217 households). This greater pattern diversity suggests that the gas consumption signals may be inherently more challenging for training prediction models compared to the electricity consumption case.

As shown in Fig. 4, the proportions of outliers are approximately 18.0% and 2.3% in the electricity and gas data, respectively. We note that the number of such outlier households is relatively small compared to the entire population, which suggests that households without resident changes in real-world data largely adhere to the consistency assumption.

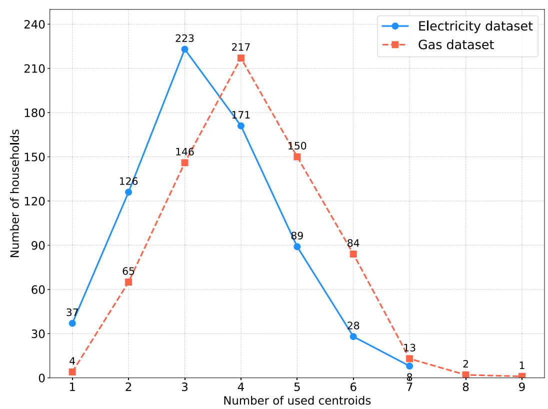

FIGURE 4. Comparison of pattern diversity histograms for the electricity and gas consumption. 37 households show a high degree of consistency in their electricity consumption, as the number of used centroids is 1.

The pattern diversity of electricity consumption can be observed in Fig. 5. Fig. 5(a) shows an example of a household that adheres to the consistency assumption, exhibiting relatively low pattern diversity. Note that all 12 patterns of this household belong to the same centroid among 10 clusters. In contrast, the 12 monthly patterns of Fig. 5(b) show relatively high diversity. In this case, the 12 patterns are distributed across 7 disjoint clusters, i.e., the number of used

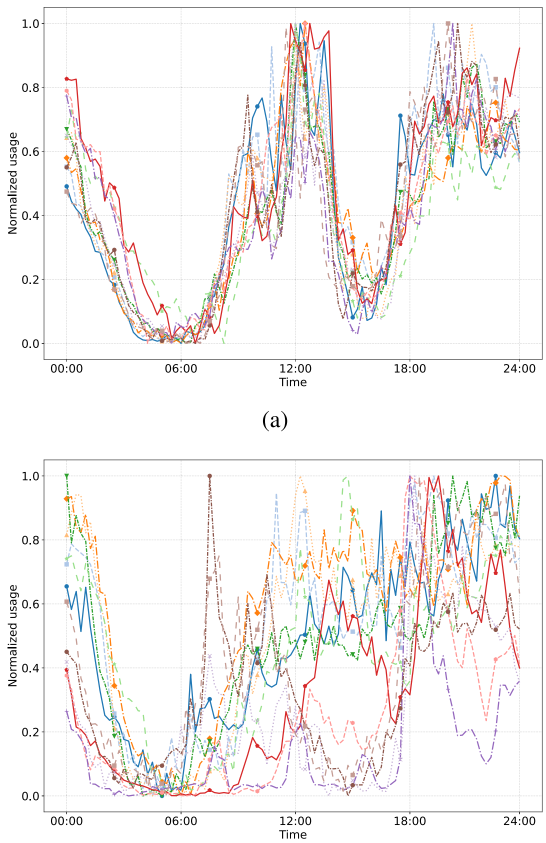

(a)

(b)

FIGURE 5. Examples of temporal pattern consistency for electricity consumption. (a) A normal household, whose 12 monthly patterns form a tight, consistent bundle. This household follows the consistency assumption. (b) An outlier household, whose monthly patterns are widely scattered and unpredictable. This household can be regarded as violating the consistency assumption.

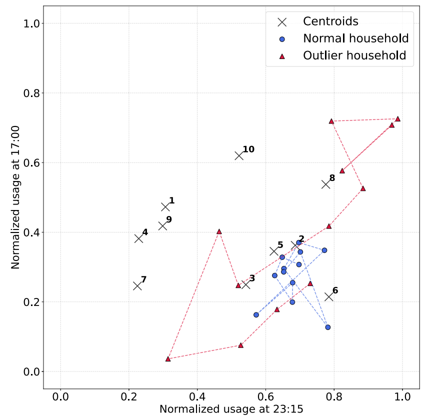

FIGURE 6. $N = 10$ centroids and the monthly patterns of the households in Fig. 5. The monthly patterns of the normal household belong to Centroid 2, with only one centroid used. In contrast, the outlier household shows patterns spread across multiple centroids, with the quantized results distributed across seven clusters. Monthly pattern points of adjacent months are connected by dotted lines.

TABLE 1. Augmented dataset for deep learning based on metered data collected in Seoul, Republic of Korea from January to December 2024. The composition and size of these datasets are the same for both electricity and gas consumption.

Dataset	Property	Number of households
Training/validation	Training (80%)	8,660
	Validation (20%)	2,165
Test	No resident change	1,255
	Resident change	1,225

centroids is 7. Hence, this household can be regarded as violating the consistency assumption. The households with patterns similar to those in Fig. 5(b) were identified as outliers and excluded because they interfere with the model's ability to learn and predict consistent patterns. In the experiments, we tested various threshold values of T_o to optimize the training performance for prediction models.

If detection is attempted on households that have been removed as outliers, they are likely to be classified as resident-change cases by the trained models. However, whereas actual resident change households exhibit inconsistency primarily in the month when the change occurs, outlier households display inconsistency across multiple months, which is a key distinction between these two categories.

To provide a more intuitive view of the centroids and actual monthly patterns, we select two elements from the 96-dimensional centroids and vectors of the monthly patterns for the households in Fig. 5. Then, we plotted them in Fig. 6 on a two-dimensional space with 10 centroids to show which centroids the monthly patterns belong to.

For the monthly amounts of the electricity and gas consumption, we did not apply an explicit outlier removal scheme, as their distributions are not widely spread.

C. PATTERN AUGMENTATION

After removing the outlier households from the dataset, data augmentation was performed to enhance data diversity and improve generalization performance [35]. Data augmentation was applied by slightly transforming the 96-dimensional vectors through multiplications with trigonometric functions, such as sine, cosine, tangent, and hyperbolic tangent. In addition, the sigmoid and Gaussian functions were also used. The degree of transformation was controlled by adjusting the amplitude of each function.

After completing the outlier exclusion and data augmentation, the entire dataset was split into training and validation datasets at a ratio of 0.8 to 0.2 for model training. Both the training and validation datasets were composed exclusively of households without resident changes. A separate test dataset was then constructed to evaluate the trained model's performance, containing an equal proportion of households with and without resident changes. This augmented dataset for the prediction model training is summarized in Table 1. Examples of the monthly patterns augmented with various functions are illustrated in Fig. 7.

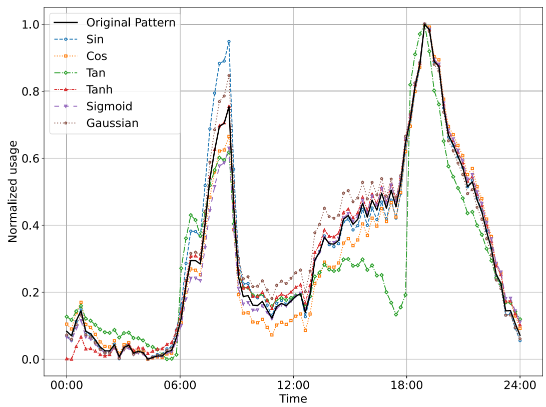

FIGURE 7. Augmentation example of the monthly pattern using six different functions.

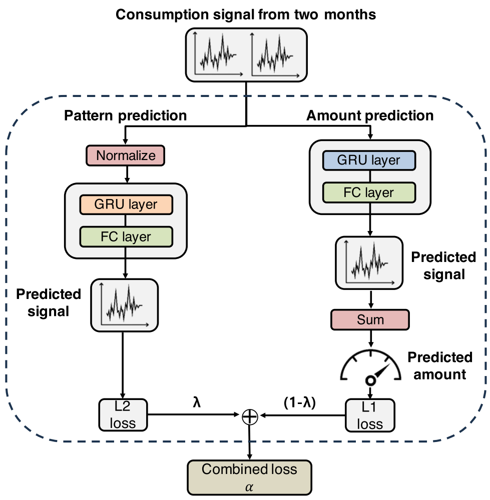

FIGURE 8. Prediction module with two GRU-FC models for the pattern and amount predictions, respectively. The L1 and L2 losses are combined into a single loss α using the weight parameter λ. Each GRU-FC model consists of four GRU layers with a hidden size of 128, followed by a single FC layer. The input is a 96 $\times$ 2-dimensional consumption signal from the previous two months and the output is a 96-dimensional vector.

III. PREDICTION AND RESIDENT CHANGE DETECTION

In this section, we describe the resident change detection method based on monthly pattern and amount prediction using deep learning.

A. DEEP LEARNING MODEL

To effectively capture the time-series characteristics of metering data, we constructed a deep learning model based on GRU, a variant of RNN. Here, GRU can overcome the limitation of the conventional RNN in capturing long-term dependencies [36], while requiring fewer parameters. For predicting monthly patterns and amounts, we employed a GRU-fully connected (FC) model, which combines GRU and FC layers.

The proposed prediction module for predicting the monthly pattern and amount of an energy source is illustrated in Fig. 8, where two separate GRU-FC models are used for pattern and amount predictions, respectively. Each prediction GRU-FC model consists of four GRU layers and one FC layer, with a hidden layer size of 128. The input to the GRU-FC model is a 96 $\times$ 2-dimensional vector, which consists of the consumption signals from the previous two consecutive months; therefore, predictions can effectively start from March. The hidden GRU layers are responsible for learning long-term dependencies and the final output, which is a prediction of the current month in the form of a 96-dimensional vector, is generated through the FC layer.

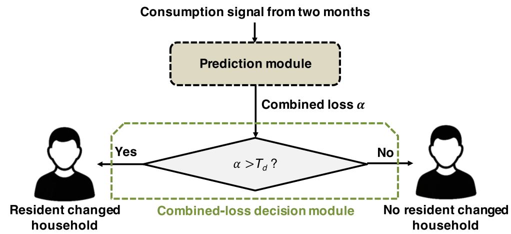

FIGURE 9. Combined-loss decision module for resident change detection using the losses α from monthly pattern and amount features. The combined losses α are calculated for each month by the prediction module in Fig. 8.

In Fig. 8, the left GRU-FC model is used for pattern prediction, receiving the patterns from the previous two months. A monthly normalization step, which is described in Subsection II-A, is applied before the model to generate the monthly patterns of the previous two months. The output is then a prediction of the current monthly pattern. The right GRU-FC model directly receives the 96 $\times$ 2-dimensional vectors in their original scale to preserve absolute usage levels and predicts a 96-dimensional vector of the consumption signal. The elements of this vector are subsequently accumulated to obtain the current monthly amount. The specific hyperparameters of the architecture, such as the number of layers and hidden layer size, were determined through empirical evaluation for each prediction model.

In training GRU-FC models, the mean squared error (L2 loss) was used as the loss function, and the Adam optimizer was employed with a drop rate of 0.3 and a batch size of 128. The learning rate was progressively adjusted from an initial learning rate of 0.001 using a cosine annealing scheduler, and the model was trained for a total of 200 epochs.

B. COMBINED-LOSS DECISION

In the proposed prediction module, both the monthly pattern and the amount of an energy source are utilized to detect the month of a resident change.

As shown in Fig. 8, the pattern and amount GRU-FC models predict the monthly pattern and amount for each month, respectively. These predictions are then compared with the actual values, and the prediction errors are calculated using the L2 and L1 losses, respectively. These losses are combined using a weight parameter λ to calculate the *combined loss* α defined as

$$\alpha := \lambda E_p + (1 - \lambda) E_a, \tag{1}$$

where E_p and E_a denote the L2 loss on the monthly pattern prediction and the L1 loss on the monthly amount prediction, respectively.

By observing α, the proposed method leverages the shift in consumption behavior to detect resident changes. When a resident change occurs, the model is tasked with predicting the new resident's first month using the last two months of the former resident's data as input. Since the new resident's patterns are unfamiliar, the model initially fails to make accurate predictions. This mismatch between the predicted and actual consumption produces a large prediction error, specifically in the month of the change. Consequently, a sharp increase in α is expected during the month of the resident change.

The overall detection process based on the combined-loss decision is illustrated in Fig. 9. For each household, the combined loss α is computed and compared against a predefined threshold T_d. If α exceeds this threshold, then that month is classified as the time of resident change for the household. We now summarize the resident change detection method based on the combined loss as follows.

Combined-Loss Decision:

0) For an energy dataset, remove outlier households and perform augmentation; set the threshold T_d.
1) Calculate the prediction losses E_p and E_a from the pattern and amount prediction models, respectively.
2) For an optimal λ_o, calculate α for each household to test the resident changes. If $\alpha > T_d$, then a resident change is detected for the corresponding month.

The combined loss α enables a simultaneous consideration of changes in both monthly pattern and amount that occur during resident changes. By adjusting λ, it is possible to balance the sensitivity between the monthly pattern and amount in detecting resident changes. An optimal weight λ_o for each month can be identified by searching for the one that maximizes the area under the curve (AUC) [37]. In (1), the L1 loss on the monthly amount is typically larger than the L2 loss on the monthly pattern. Hence, the L1 and L2 losses are min-max normalized across all months, respectively, and then combined with λ to obtain α.

In searching λ_o from the area curve, optimization can be performed using line search methods, such as the golden-section search [38, p.270] for a feasible region of [0, 1].

For each month, a threshold of $T_d = \mu + \sigma$ is considered in the simulations, where μ and σ denote the empirical mean and standard deviation of α, respectively. This threshold can be adjusted depending on the applications of the detection method. However, it is observed that the detection accuracy is not sensitive to the threshold value.

C. COMPLEMENTARY DECISION

The combined-loss decision scheme can be applied independently to the electricity and gas datasets, yielding separate detection results for each energy source. For the final decision, we can employ a complementary approach: a resident change is flagged if either the electricity-based scheme or the gas-based scheme detects a change as shown in Fig. 10. This *complementary decision* scheme leverages the distinct characteristics of each energy dataset. Specifically, a change in appliance usage might be evident only in the electricity consumption data, whereas a shift in heating habits may be captured primarily by the gas consumption data.

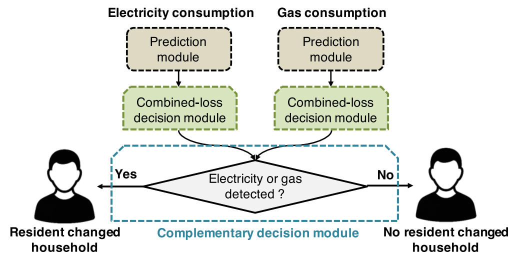

FIGURE 10. Complementary decision module for resident change detection using the combined-loss decisions from electricity and gas consumption.

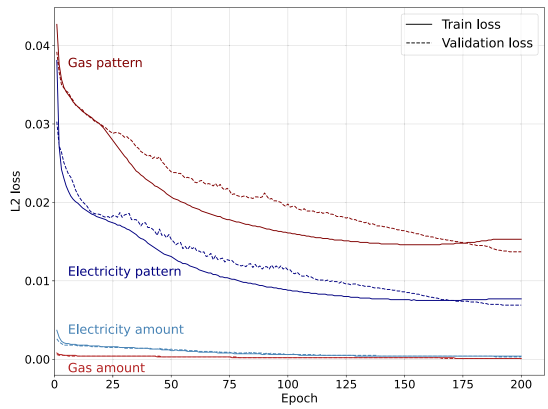

FIGURE 11. Training and validation loss curves for the prediction models.

D. SHIFT IN DETECTION

The dataset used in this paper contains labels indicating the date on which a household moved. It is noted that when detecting resident changes on a monthly basis, there could be an inherent discrepancy between the actual moving date and the detected month, as explained below. Considering this discrepancy, we introduce the concept of extending the error margin when detection is performed on a monthly basis.

If a resident change occurs in the middle or at the end of a month, the consumption data for that month will be a mixture of patterns of both the former and new residents. This mixed signal can be ambiguous and difficult to interpret. The distinct and complete consumption pattern of the new resident, however, becomes fully apparent in the data of the following month. Therefore, allowing a +1-month margin can account for these cases where the definitive evidence of a change is most clearly reflected in the subsequent month data.

Conversely, an error margin of −1 month is important for accounting for significant shifts in consumption that occur in the month immediately preceding the official resident change. Our analysis revealed that some households exhibit a unique transitional pattern during this pre-move period, which belongs to neither the former nor the new resident. In the electricity data, this transitional pattern is characterized by low-magnitude consumption concentrated exclusively during daytime hours, with usage dropping to near zero in the mornings and evenings. Similarly, the corresponding gas consumption for this same period typically drops to near zero. All of these patterns indicate a pre-move preparation period, such as renovation. This observation plausibly corresponds to scenarios where new residents undertake renovations before officially taking up residence.

Given these practical considerations, allowing an error margin of ± 1 month is a reasonable evaluation approach that reflects the realistic characteristics of resident changes. All subsequent simulations are performed using this error margin.

IV. SIMULATION RESULTS

In this section, we first present the simulations conducted to design the prediction models and the combined-loss decision scheme. We then provide the simulation results evaluating the performance of the resident change detection method including the complementary decision scheme.

A. IMPLEMENTATION OF THE DETECTION METHOD

Fig. 11 illustrates the training and validation loss curves of the GRU-FC models used for the pattern and amount predictions, which were implemented using Python 3.11.4 and PyTorch. Because the number of learnable hyperparameters is relatively small, the models did not require substantial computational resources or training time. Both the electricity and gas prediction models converged with relatively low loss values, indicating stable training. We can observe that the pattern prediction models exhibited more distinct learning dynamics. Notably, the gas pattern model consistently showed higher losses than the electricity pattern model, both at the initial epochs and at convergence. This difference reflects the greater pattern diversity previously observed in the gas dataset, as shown in Fig. 5(b).

Fig. 12 shows an example of determining the optimal weight parameter λ_o for May. For each energy type, the values of AUC are plotted against different values of λ. The optimal λ_o values for the electricity and gas datasets are found to be 0.90 and 0.65, respectively, where the AUC values are maximized. For electricity, the relatively high weight parameter of 0.90 indicates that the pattern is the dominant feature, whereas for gas, the more balanced value of 0.65 suggests that the monthly amount also serves as a meaningful complementary feature. For the electricity dataset, varying the weight parameter within the range [0.65, 1.00] results in a change in AUC of approximately 1.0%. For the gas dataset, varying the weight parameter within the range [0.40, 0.90] leads to a change in AUC of approximately 1.2%. Hence, we observe that the detection performance is not overly sensitive to variations in the weight parameters and remains robust.

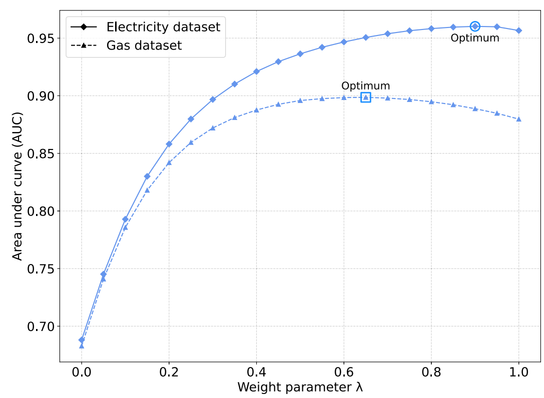

FIGURE 12. Optimization of the weight parameter λ in May for electricity and gas.

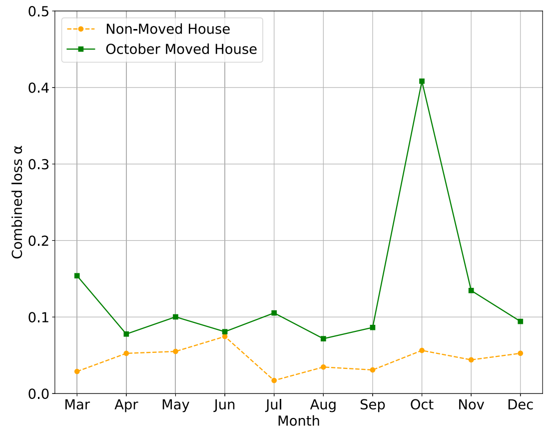

FIGURE 13. Comparison of the monthly combined loss α for a household without a resident change and one with a change in October.

An example of detection using the combined loss α is illustrated in Fig. 13. For households without resident changes, their consumption behavior remains constant throughout the year, according to the consistency assumption. In other words, their monthly patterns and amounts are less variable, making predictions easier. Hence, these households exhibit low values of α. In contrast, for a household with a resident change in October, α shows a sharp peak in that month before decreasing again as the prediction model adapts to the new patterns.

B. DETECTION PERFORMANCE

To quantitatively assess detection performance, we employed several evaluation metrics including accuracy, precision, specificity, and recall, all derived from the confusion matrix, along with AUC.

We now introduce and compare the simulation results for the proposed resident change detection method. Several detection methods employing different combinations of the

TABLE 2. Performance comparison under various configurations of the proposed resident change detection method. The thresholds T_o used for the outlier removal are 4 and 6 for the monthly pattern and amount, respectively.

	Method 1		Method 2		Method 3		Method 4		Method 5
	Electricity		Gas		Complementary Electricity & gas		Combined-loss Pattern & amount		Combined-loss & complementary
	Pattern	Amount	Pattern	Amount	Pattern	Amount	Electricity	Gas	All features
Accuracy	76.61	70.53	76.37	62.12	86.20	71.35	80.37	76.33	89.18
Precision	98.95	92.84	96.68	70.52	97.03	76.33	99.47	96.67	97.43
Specificity	99.43	96.54	98.12	82.53	97.71	80.82	99.67	98.12	97.88
Recall	53.80	44.49	54.61	41.80	74.69	61.88	61.06	54.53	80.49

The unit is %

features are considered and the simulation results are summarized in Table 2 for their performance comparison. Here, the thresholds T_o for the outlier removal are 4 and 6 for the monthly pattern and amount, respectively. The configurations in Methods 1 and 2 use a single feature without applying either the combined-loss or complementary decision modules. Method 3 uses both electricity and gas datasets with the complementary decision modules, but without the combined-loss decision shown in Fig. 9. The method labeled 'Pattern' in Methods 1-3 of Table 2 uses only the left model of the prediction module in Fig. 8 ($\lambda = 1$). Similarly, the method labeled 'Amount' uses only the right model ($\lambda = 0$). Method 4 uses both monthly pattern and amount features based on the combined-loss decision, with the prediction module shown in Figs. 8 and 9, but without employing the complementary decision module. The method labeled 'Electricity' uses only the electricity feature and the method labeled 'Gas' uses only the gas feature. Method 5 receives both the electricity and gas features using the two prediction modules shown in Fig. 8. The combined-loss decision outputs from both electricity and gas prediction modules are then passed to the complementary decision step to make the final resident change decision. Note that Method 5 uses all available features: the monthly pattern and amount of electricity consumption, as well as those of gas consumption.

From the results of Methods 1, 2, and 3 in Table 2, we observe that detection using the monthly pattern is significantly more effective than detection using only the monthly amount. In other words, the monthly pattern is the dominant feature for detecting resident changes compared to the monthly amount. Detection using only electricity consumption outperforms detection using only gas consumption, as shown by the results on Methods 1, 2, and 4. Note that the monthly patterns of gas are considerably noisy, as shown in Fig. 2, making it more difficult to distinguish the distinct signal of a resident change from the inherent noise in the patterns. Method 5, which uses all features, achieves the best detection results. When using only electricity data, the detection accuracy was 80.37%; however, when electricity and gas datasets were used together, the detection accuracy significantly improved to 89.18%.

Note that we used real-world datasets collected from actual environments for both model training and detection. Hence, we expect that the proposed method will also exhibit robust detection performance when applied to other real-world datasets.

V. DISCUSSIONS

In this section, we first discuss the various causes of detection errors and examine examples of problems caused by detection shifts. We then discuss the effect of the outlier removal on training the prediction models.

A. DETECTION FAILURES

Detection failures fall into two categories: failing to detect an actual resident change (false negative) and incorrectly flagging a change when none occurred (false positive).

From a false negative perspective, an actual resident change may be missed if the energy consumption behavior of new residents is very similar to that of previous residents. Consequently, α remains insufficient to exceed the threshold, as the behavioral shift is too small to generate a discernible signal. In most cases of Methods 1 through 4, the recall values are relatively low, which implies that the false negative rate is relatively high.

From a false positive perspective, a detection failure may also occur when a resident change is incorrectly flagged in a household where none has occurred. This error is most prevalent when consumption behavior is inherently erratic and unpredictable. For example, household demographic transitions, such as a change in the number of occupants or family type, can have a measurable impact on domestic energy usage [39]. These transitions often lead to an increase in energy consumption, creating a distinct shift in the time-series data. For instance, a significant change in consumption can also occur when a co-resident with a different lifestyle moves in. In addition, as another example, the number of residents who telecommute has increased due to the COVID-19 pandemic, and they exhibit distinctly different consumption patterns, including a substantial increase in daytime energy use [40]. In such households, an atypical consumption pattern in a specific month can cause α to spike sharply, leading the model to incorrectly interpret a temporal deviation in existing resident behavior as a resident change. These failure modes illustrate an operational characteristic of prediction-based resident change detection. Note that the consistency

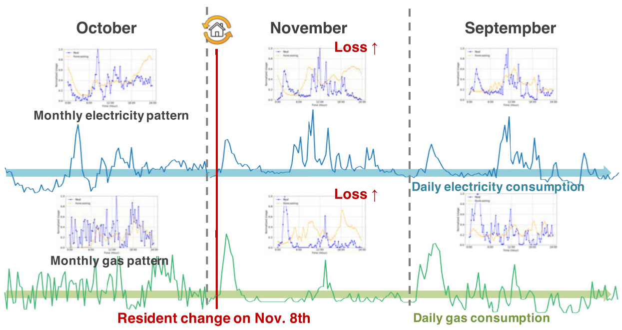

FIGURE 14. Example of the electricity and gas consumption signals. The resident change occurred on November 8th, 2024, the beginning of the month. The resident change is correctly detected.

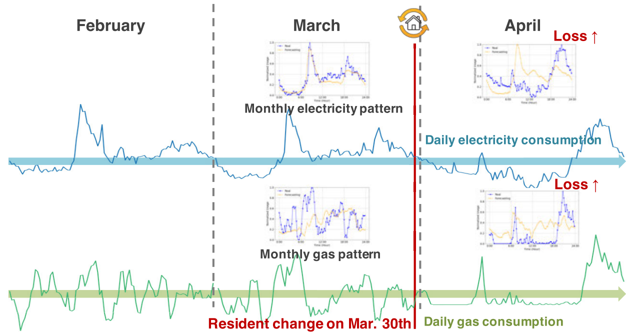

FIGURE 15. Example of the electricity and gas consumption signals. The resident change occurred on March 30th, 2024, the end of the month. The resident change was detected a month later in April (detection shift of +1).

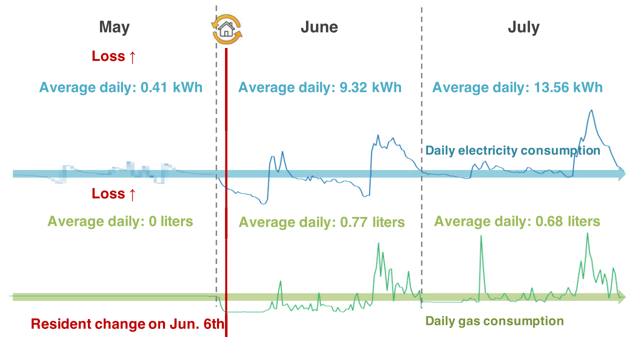

FIGURE 16. Example of the electricity and gas consumption signals. The resident change occurred on June 6th, 2024, the beginning of the month. Before the resident change, electricity and gas consumption were very low. The resident change was detected in May, one month earlier (detection shift of −1).

assumption does not hold for these households, as mentioned in Subsection II-B.

Because the detection is performed on a monthly basis, short-term variations in consumption due to holidays or weekends are largely averaged out and the risk of false positives from such events is small. However, if a resident is absent for an extended period longer than one month, this situation may be falsely detected as a resident change.

Similarly, changes in consumption caused by appliance failures or acquisition of new appliances are expected to have only a minor impact when detection is performed on a monthly basis. However, changes in the use of high-consumption appliances, such as air conditioners, induction cooktops, or hair dryers, can noticeably alter electricity consumption patterns and may act as a source of false positives. In addition, if appliance failures occur frequently, the resulting irregular usage can increase pattern diversity. In such cases, these households may be regarded as outliers and excluded from the training dataset.

Multi-year datasets collected from regions with climates or geographical characteristics substantially different from Seoul may limit the generalizability of the proposed method. In such cases, an approach that fine-tunes the model using techniques such as transfer learning could be used.

Therefore, when deploying the proposed method in real-world settings, extending the framework to explicitly model and account for such additional anomalies can be considered an important direction for future research.

B. DETECTION SHIFT AND THE ERROR MARGIN

Because the detection resolution is monthly, detection shifts may occur when comparing changes on a daily basis, as described in Subsection III-D. Fig. 14 shows a correctly detected case, where the resident change occurred at the beginning of the month. Fig. 15 shows a case with +1 shift, where the resident change occurred at the end of the month. Fig. 16 shows a case with −1 shift.

TABLE 3. Performance of the resident change detection depending on the error margin. The simulation results were obtained for Method 5. The thresholds T_O in the outlier removal are 4 and 6 for the monthly pattern and amount, respectively.

	No error margin	±1-month error margin
Accuracy	69.06	89.18
Precision	94.99	97.43
Specificity	97.88	97.88
Recall	40.24	80.49
AUC	99.26	99.26

The unit is %

To solve this detection shift problem, a margin is provided. We now observe the improved detection performance achieved by using the error margin ±1-month. The simulation results with and without the error margin are summarized for comparison in Table 3. The accuracy of 69.06% without considering the margin of error improves significantly to 89.1% when allowing for the ±1-month error margin. We can also observe in Table 3 that the detection method demonstrates high precision and specificity values under both evaluation settings. However, the overall accuracy and recall values vary considerably depending on whether the margin of error is applied.

TABLE 4. Performance comparison for different combinations of T_o in the outlier removal. The simulation results were obtained for Method 5.

	Outlier threshold T_o				Without outlier removal
Electricity	4	4	5	5	
Gas	5	6	5	6	
Accuracy	87.76	89.18	86.12	87.06	61.14
Precision	97.44	97.43	97.33	96.61	62.67
Specificity	97.96	97.88	97.96	97.31	67.18
Recall	77.55	80.49	74.29	76.82	55.10

The unit is %

C. OUTLIER REMOVAL

As discussed in Subsection II-B, removing the outlier households that do not follow the consistency assumption is important for training the prediction models based on GRU-FC. To examine the effect of the outlier removal on the training performance, we conducted simulations for different combinations of the threshold T_o for the electricity and gas data. The simulation results are summarized in Table 4. Considering the maximum accuracy values, we can observe that the optimal thresholds for T_o are 4 and 6 for electricity and gas, respectively. Without outlier removal, the accuracy is 61.14%; however, with outlier removal applied, the accuracy increases to 89.18%.

D. DEPLOYMENT OF THE DETECTION METHOD

We propose to deploy the detection framework in the data concentration unit (DCU), which is the local data collection hub of the AMI architecture as shown in Fig. 1. By utilizing the DCU's computing power, resident changes can be detected at the ''edge'' before the data is transmitted to the central metering data management system. Processing data locally on the DCU minimizes the exposure of raw and high-resolution energy consumption data to external cloud systems, thereby enhancing the protection of residents' personal information. As discussed in Subsection IV-A, our GRU-FC model is lightweight and does not require substantial computational resources. This makes it feasible to run on the embedded processors typically found in modern DCUs. AMI equipment manufacturers and utility companies would be the primary adopters, integrating this detection logic as a built-in ''privacy-by-design'' feature of the DCU hardware. This approach reduces the operational burdens, cloud storage, and processing costs for utility providers.

VI. CONCLUSION

In this paper, we proposed an unsupervised framework for detecting resident changes using a deep learning prediction model based on GRU-FC. This framework estimates monthly resident changes by analyzing prediction errors in consumption patterns and amounts from 15-minute-resolution electricity and gas metering datasets collected from 750 real-world households with ground-truth labels for resident change dates. To prepare the dataset for training the GRU-FC models, an efficient outlier removal scheme was developed based on VQ. Combined-loss and complementary decision schemes were employed to jointly leverage pattern and amount features for both electricity and gas data. When using only electricity data, the detection accuracy was 80.37%; however, when electricity and gas datasets were used together, the detection accuracy significantly improved to 89.18%.

ACKNOWLEDGMENT

(Jongin Kim and Dong Sik Kim contributed equally to this work.)

REFERENCES

[1] M. Mahmood, P. Chowdhury, R. Yeassin, M. Hasan, T. Ahmad, and N.-U.-R. Chowdhury, ''Impacts of digitalization on smart grids, renewable energy, and demand response: An updated review of current applications,'' *Energy Convers. Manage., X*, vol. 24, Oct. 2024, Art. no. 100790.

[2] Y. Kim, N.-G. Myoung, and S.-Y. Lee, ''Study on AMI system of KEPCO,'' in *Proc. Int. Conf. Inf. Commun. Technol. Converg. (ICTC)*, Nov. 2010, pp. 459–460.

[3] D. S. Kim, B. J. Chung, and Y. M. Chung, ''Statistical learning for service quality estimation in broadband PLC AMI,'' *Energies*, vol. 12, no. 4, p. 684, Feb. 2019.

[4] D. S. Kim, B. J. Chung, and Y. M. Chung, ''Analysis of AMI communication methods in various field environments,'' *Energies*, vol. 13, no. 19, p. 5185, Oct. 2020.

[5] J. S. Guerrero-Prado, W. Alfonso-Morales, E. Caicedo-Bravo, B. Zayas-Pérez, and A. Espinosa-Reza, ''The power of big data and data analytics for AMI data: A case study,'' *Sensors*, vol. 20, no. 11, p. 3289, Jun. 2020.

[6] D. S. Kim, S.-Y. Son, and J. Lee, ''Developments of the in-home display systems for residential energy monitoring,'' *IEEE Trans. Consum. Electron.*, vol. 59, no. 3, pp. 492–498, Aug. 2013.

[7] T. Yu, D. S. Kim, and S.-Y. Son, ''Optimization of scheduling for home appliances in conjunction with renewable and energy storage resources,'' *Int. J. Smart Home*, vol. 7, no. 4, pp. 261–272, 2013.

[8] G. Ruan, D. Qiu, S. Sivaranjani, A. S. A. Awad, and G. Strbac, ''Data-driven energy management of virtual power plants: A review,'' *Adv. Appl. Energy*, vol. 14, Jul. 2024, Art. no. 100170.

[9] K. McKenna, P. Gotseff, M. Chee, and E. Ifuku, ''Advanced metering infrastructure for distribution planning and operation: Closing the loop on grid-edge visibility,'' *IEEE Electrific. Mag.*, vol. 10, no. 4, pp. 58–65, Dec. 2022.

[10] J. Peppanen, M. J. Reno, M. Thakkar, S. Grijalva, and R. G. Harley, ''Leveraging AMI data for distribution system model calibration and situational awareness,'' *IEEE Trans. Smart Grid*, vol. 6, no. 4, pp. 2050–2059, Jul. 2015.

[11] A. Althobaiti, C. Rotsos, and A. K. Marnerides, ''Adaptive energy theft detection in smart grids using self-learning with dual neural network,'' *IEEE Trans. Ind. Informat.*, vol. 20, no. 2, pp. 2776–2786, Aug. 2023.

[12] X.-Y. Zhang, P. Guo, S. Kuenzel, and C. Yin, ''Ethical considerations in advanced metering infrastructure integration: A systematic review,'' *Energy Strategy Rev.*, vol. 56, Nov. 2024, Art. no. 101571.

[13] C. Chen, Z. Xie, L. Wang, Y. Xie, G. Geng, and H. Yu, ''Anomaly detection of pollution control equipment based on AMI data analytics,'' in *Proc. IEEE Int. Conf. Power Syst. Technol. (POWERCON)*, Sep. 2020, pp. 1–6.

[14] A. J. Almalki, ''Unsupervised learning with hybrid models for detecting electricity theft in smart grids,'' *IEEE Access*, vol. 12, pp. 187027–187040, 2024.

[15] A. H. M. Jakaria, M. A. Rahman, and M. G. Moula Mehedi Hasan, ''Safety analysis of AMI networks through smart fraud detection,'' in *Proc. IEEE Conf. Commun. Netw. Secur. (CNS)*, Jun. 2019, pp. 1–7.

[16] A. M. Al-Ghaili, Z.-.-A. Ibrahim, S. A. S. Hairi, F. A. Rahim, H. Baskaran, N. A. M. Ariffin, and H. Kasim, ''A review of anomaly detection techniques in advanced metering infrastructure,'' *Bull. Electr. Eng. Informat.*, vol. 10, no. 1, pp. 266–273, Feb. 2021.

[17] Y. Peng, Y. Yang, Y. Xu, Y. Xue, R. Song, J. Kang, and H. Zhao, ''Electricity theft detection in AMI based on clustering and local outlier factor,'' *IEEE Access*, vol. 9, pp. 107250–107259, 2021.

[18] Q. Zhao, Z. Chang, and G. Min, "Anomaly detection and classification of household electricity data: A time window and multilayer hierarchical network approach," *IEEE Internet Things J.*, vol. 9, no. 5, pp. 3704–3716, Mar. 2022.

[19] W. Zhou, B. Li, H. Xiao, H. Xiao, W. Wang, Y. Zheng, and S. Su, "Electricity theft detection of residential users with correlation of water and electricity usage," *IEEE Trans. Ind. Informat.*, vol. 20, no. 4, pp. 5339–5351, Apr. 2024.

[20] W. Liao, R. Zhu, Y. Yang, Y. Jia, Z. Yang, and C. Rehtanz, "Electricity theft detection with multi-source data: Integrating electricity, water, and gas," *IEEE Trans. Ind. Appl.*, vol. 62, no. 2, pp. 3187–3197, Mar./Apr. 2025.

[21] Y. Himeur, K. Ghanem, A. Alsalemi, F. Bensaali, and A. Amira, "Artificial intelligence based anomaly detection of energy consumption in buildings: A review, current trends and new perspectives," *Appl. Energy*, vol. 287, Apr. 2021, Art. no. 116601.

[22] S. Lee, H. Jin, S. H. Nengroo, Y. Doh, C. Lee, T. Heo, and D. Har, "Smart metering system capable of anomaly detection by bi-directional LSTM autoencoder," in *Proc. IEEE Int. Conf. Consum. Electron. (ICCE)*, Jan. 2022, pp. 1–6.

[23] X. Gong, S. Liao, F. Hu, X. Hu, and C. Liu, "Autoencoder-based anomaly detection for time series data in complex systems," in *Proc. IEEE Asia–Pacific Conf. Circuits Syst. (APCCAS)*, Nov. 2022, pp. 428–433.

[24] X. Zhao, W. Chen, Q. Yin, B. Wang, Z. Li, and J. Wang, "Bidirectional deep variational RNN for refining anomaly detection of multivariate time series," in *Proc. IEEE 10th Joint Int. Inf. Technol. Artif. Intell. Conf. (ITAIC)*, vol. 10, Jun. 2022, pp. 1504–1509.

[25] Y. Choi, H. Lim, H. Choi, and I.-J. Kim, "GAN-based anomaly detection and localization of multivariate time series data for power plant," in *Proc. IEEE Int. Conf. Big Data Smart Comput. (BigComp)*, Feb. 2020, pp. 71–74.

[26] P. Malhotra, A. Ramakrishnan, G. Anand, L. Vig, P. Agarwal, and G. Shroff, "LSTM-based encoder–decoder for multi-sensor anomaly detection," 2016, *arXiv:1607.00148*.

[27] K. Hundman, V. Constantinou, C. Laporte, I. Colwell, and T. Soderstrom, "Detecting spacecraft anomalies using LSTMs and nonparametric dynamic thresholding," in *Proc. 24th ACM SIGKDD Int. Conf. Knowl. Discovery Data Mining*, Jul. 2018, pp. 387–395.

[28] D. S. Kim, "Finding the number of clusters using a small training sequence," *IEEE Access*, vol. 11, pp. 25932–25940, 2023.

[29] R. L. Thorndike, "Who belongs in the family?" *Psychometrika*, vol. 18, no. 4, pp. 267–276, Dec. 1953.

[30] C. A. Sugar and G. M. James, "Finding the number of clusters in a dataset," *J. Amer. Stat. Assoc.*, vol. 98, no. 463, pp. 750–763, Sep. 2003.

[31] P. J. Rousseeuw, "Silhouettes: A graphical aid to the interpretation and validation of cluster analysis," *J. Comput. Appl. Math.*, vol. 20, no. 1, pp. 53–65, 1987.

[32] R. Tibshirani, G. Walther, and T. Hastie, "Estimating the number of clusters in a data set via the gap statistic," *J. Roy. Stat. Soc. Ser. B, Stat. Methodol.*, vol. 63, no. 2, pp. 411–423, Jul. 2001.

[33] A. Gersho and R. M. Gray, *Vector Quantization and Signal Compression*. Boston, MA, USA: Kluwer, 1992.

[34] D. S. Kim and M. R. Bell, "Upper bounds on empirically optimal quantizers," *IEEE Trans. Inf. Theory*, vol. 49, no. 4, pp. 1037–1046, Apr. 2003.

[35] Z. Gao, H. Liu, and L. Li, "Data augmentation for time-series classification: An extensive empirical study and comprehensive survey," *J. Artif. Intell. Res.*, vol. 83, pp. 5:1–5:46, Jun. 2025.

[36] H. Hewamalage, C. Bergmeir, and K. Bandara, "Recurrent neural networks for time series forecasting: Current status and future directions," *Int. J. Forecasting*, vol. 37, no. 1, pp. 388–427, Jan. 2021.

[37] A. F. Emmott, S. Das, T. Dietterich, A. Fern, and W.-K. Wong, "Systematic construction of anomaly detection benchmarks from real data," in *Proc. ACM SIGKDD Workshop Outlier Detection Description*, Aug. 2013, pp. 16–21.

[38] M. S. Bazaraa, *Nonlinear Programming, Theory and Algorithms*, 2nd ed., Hoboken, NJ, USA: Wiley, 1993.

[39] B. Medjdoub and M. L. Chalal, "Impact of household transitions on domestic energy consumption and its applicability to urban energy planning," *Frontiers Eng. Manage.*, vol. 4, no. 2, pp. 171–183, 2017.

[40] M. Kojima and T. Saito, "COVID-19 triggered residential behavioral changes and electricity consumption of detached houses in Japan," *Energy Buildings*, vol. 290, Jul. 2023, Art. no. 113082.

JONGIN KIM (Student Member, IEEE) is currently pursuing the M.S. degree with the Division of Semiconductor and Electronics Engineering, Hankuk University of Foreign Studies, Republic of Korea. His research interests include biomedical image processing and medical physics based on machine learning and statistical signal processing.

DONG SIK KIM (Senior Member, IEEE) received the B.S., M.S., and Ph.D. degrees in electrical engineering from Seoul National University, Seoul, Republic of Korea, in 1986, 1988, and 1994, respectively. Since 1986, he has been the Research Director with Automan Company Ltd., Republic of Korea, where he has conducted RF circuit design projects. From 1998 to 1999, he was a Visiting Assistant Professor with the School of Electrical and Computer Engineering, Purdue University, West Lafayette, IN, USA. He is currently a Professor with the Division of Semiconductor and Electronics Engineering, Hankuk University of Foreign Studies, Republic of Korea. His research interests include the theory of quantization, biomedical image processing, medical physics, sensor networks, and smart grids based on statistical signal processing. He was a co-recipient of the 2003 International Workshop on Digital Watermarking Best Paper Prize.

YOUNG MO CHUNG (Member, IEEE) received the B.S., M.S., and Ph.D. degrees in electrical engineering from Seoul National University, Seoul, Republic of Korea, in 1986, 1988, and 1993, respectively. From 1994 to 1995, he was with the Engineering Research Center for Control and Instrumentation, Seoul National University, engaged in the development of digital wireless systems. In 1995, he joined the Department of Electronics and Information Engineering, Hansung University, Seoul, where he is currently a Professor. From August 1998 to July 1999, he was a Postdoctoral Fellow with the Wireless Systems Laboratory, Georgia Institute of Technology, Atlanta, GA, USA. From July 2005 to August 2006, he was a Visiting Professor with the School of Electrical Engineering and Computer Science, Oregon State University, Corvallis, OR, USA. His research interests include wireless communications, power line communications, and smart grids.

BEOM JIN CHUNG received the B.S. and M.S. degrees from Seoul National University, Seoul, Republic of Korea, in 1986 and 1988, respectively, and the Ph.D. degree from the Hankuk University of Foreign Studies, Republic of Korea, in 2014. From 2008 to 2018, he was with the Smart Green Home Research Center, Gachon University, engaged in the research of the smart grids. In 2019, he joined the Research Center of Electrical and Information Technology, Seoul National University of Science and Technology, Seoul, where he is currently a Research Professor. His research interests include the smart grids, smart metering, AMI communication networks, and electric vehicle charging systems.